

## Non-Inductive Improved H-mode Operation in ASDEX Upgrade

A. Bock, E. Fable, R. Fischer, M. Reich, D. Rittich, J. Stober,  
 M. Bernert, A. Burckhart, M. Dunne, B. Geiger, L. Giannone, A. Kappatou, O. Maj,  
 R. McDermott, A. Mlynek, E. Poli, G. Tardini, H. Zohm and the ASDEX Upgrade Team  
*Max-Planck-Institut für Plasmaphysik, D-85748 Garching, Germany*

### Introduction

Tokamak operation is constrained in several ways. For instance, aside from being susceptible to deleterious magnetohydrodynamic (MHD) instabilities like Neoclassical Tearing Modes (NTMs) or sawteeth, the conventional tokamak operation in high-confinement mode also depends on inductive current from the central solenoid to maintain the plasma current. This restricts conventional tokamaks to pulsed operation with finite pulse lengths.

One way to alleviate these drawbacks is to manipulate the plasma current profile using external means such that the safety factor  $q$  remains above 1.5, thereby eliminating the flux surfaces with rational  $q$  values like 1 or 1.5. Consequently, sawteeth and the most common NTMs with helicities up to and including  $m/n = 3/2$  are avoided, which improves the discharge stability and confinement. Furthermore, the elevated  $q$  and thus reduced poloidal magnetic field  $B_{\text{pol}}$  lead to an increase of the bootstrap current  $j_{\text{bs}} \propto \nabla p / B_{\text{pol}}$ , which minimises the dependence on inductive current and thus extends the pulse lengths.

Previous investigations in larger devices like JET or JT-60U have achieved elevated  $q$ -profiles with improved confinement using early heating during the current ramp-up, albeit only transiently [1, 2]. Recent results from DIII-D demonstrate successful high confinement, steady-state operation at  $q_{95} \approx 5$  and  $H_{\text{IPB98}(y,2)} \approx 1.4$  using early heating and on-axis electron-cyclotron current drive (ECCD) [3]. This contribution extends these studies towards steady state operation with improved confinement and high non-inductive current fraction in the full-tungsten tokamak ASDEX Upgrade (AUG) [4].

### Equilibrium Reconstruction

In order to study advanced scenarios, an accurate determination of the plasma equilibrium, and in particular its  $q$ -profile, is essential. The equilibrium is reconstructed with a novel equilibrium reconstruction code based on integrated data analysis (IDE) [5, 6], using all available data. Here, data from Faraday rotation polarimetry and Motional Stark Effect (MSE) polarimetry are essential. The MSE diagnostic was found to be susceptible to interference from polarised background light, which was attributed to initially unpolarised light from phenomena like bremsstrahlung or molecular emissions that is reflected into the MSE view by the reflective tungsten walls, thereby picking up a polarisation.

In principle, the polarisation angle measurements of a pair of adjacent MSE views that observe the  $\pi$  and  $\sigma$  emissions should be  $\Delta\gamma_m = 90^\circ$  apart. The correlations shown in figure 1

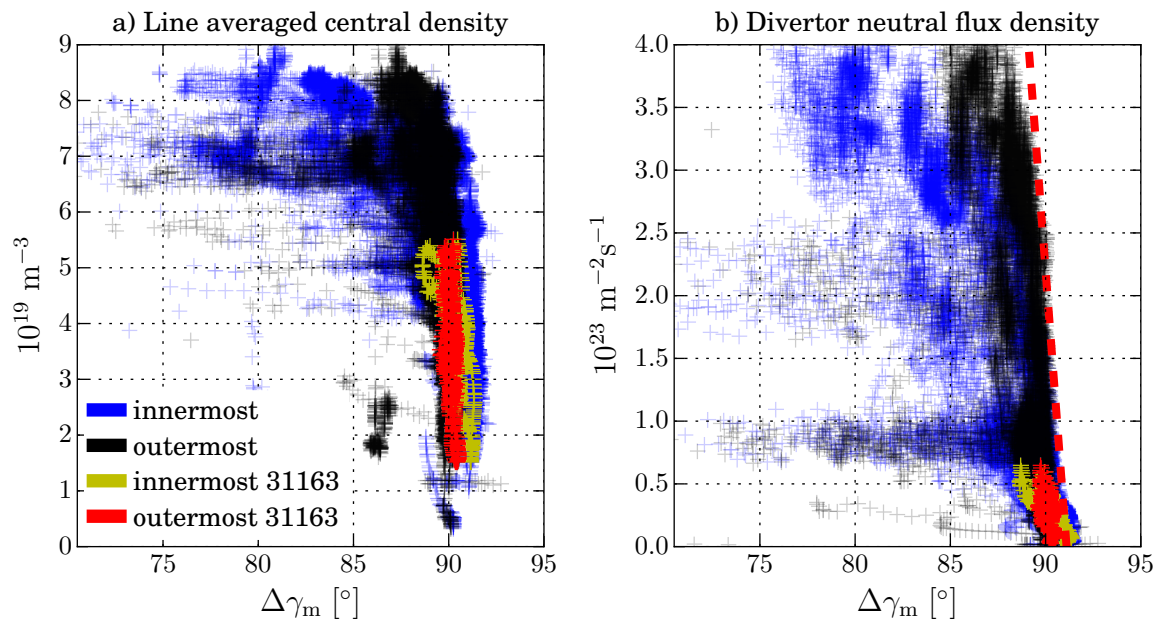


Figure 1: Dependence of the difference between two adjacent views of MSE measurements on a) line averaged central density (H-1) and b) divertor neutral flux density. Data are from several hundred AUG discharges for the radially innermost and outermost pairs. Points for discharge 31163 indicate the operational space of the studies presented here. See below for more details.

indicate that the measurements can be severely compromised with a) increasing density and b) increasing divertor neutral flux density. The latter, in particular, forms a hard limit for the MSE accuracy, shown as a dashed line in figure 1b). These observations are in line with similar findings from the C-Mod tokamak [7], where a system to compensate for the polarised background has been installed. A prototype system for AUG based on C-Mod's is currently in development.

Following these results, the systematic errors of the MSE for the studies presented here are estimated to  $\Delta\gamma \approx \pm 0.3^\circ$ , limiting the accuracy of the equilibrium reconstruction to  $\Delta q \approx \pm 0.2$ .

### Non-Inductive Operation

In a discharge with  $I_p = 800$  kA,  $B_t = -2.5$  T,  $|q_{95}| \approx 5.3$  initial tailoring of the  $q$ -profile is accomplished by redistributing current from the centre towards the edge using ECCD and neutral beam current drive (NBCD), both off-axis, followed by a feedback-controlled increase of neutral beam power to reach and maintain  $\beta_N = 2.7$  for approximately 1.5 s as shown in figure 2a). The initial external manipulation of  $q$  leads to an increase of bootstrap current such that during this high- $\beta$  phase over 95% of the toroidal plasma current can be attributed to non-inductive current (cf. figure 2b). For machine protection, the length of this phase was initially limited to only about one resistive time  $\tau_R$ , although extended phases  $>2\tau_R$  have also been realised subsequently [8]. Further extension is necessary to judge the scenario's potential for stationarity as the current profile continues to evolve slightly. Figure 2d) shows the individual

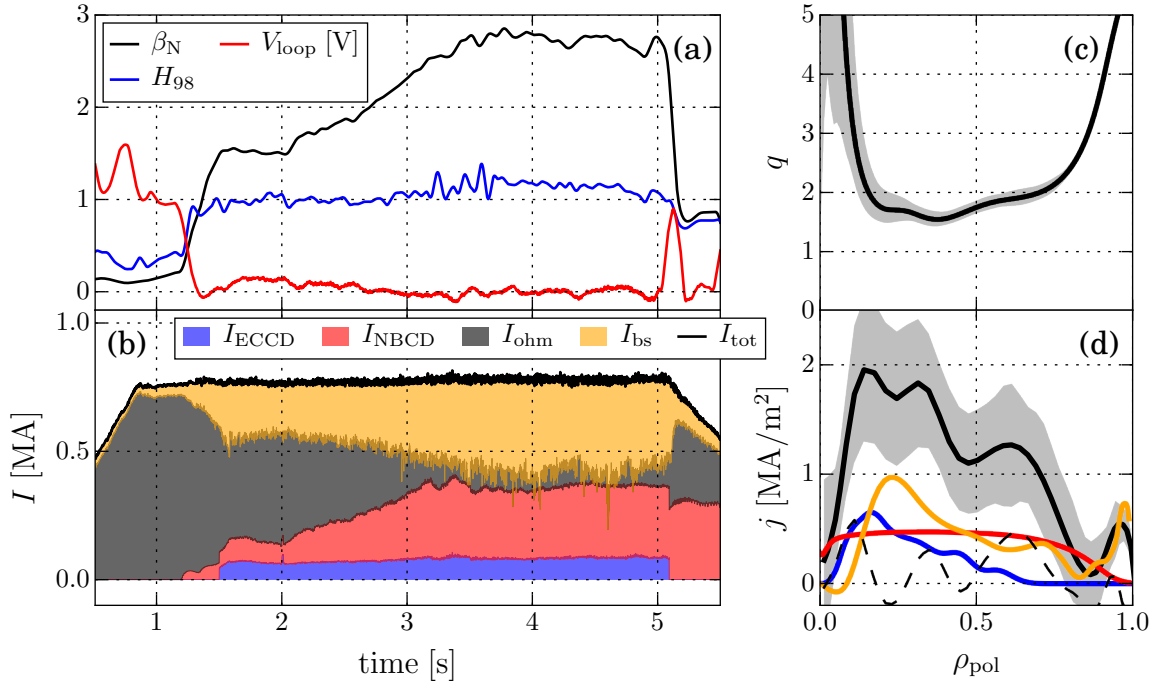


Figure 2: Key quantities for discharge 32305: a)  $\beta_N$ ,  $H_{\text{IPB98}(y,2)}$  and loop voltage  $V_{\text{loop}}$ ; b) composition of toroidal current; c) average  $q$ -profile between 3.5 and 4.5 s; d) modelled and reconstructed toroidal current density profiles in the same interval (see text for more details).

contributions to the toroidal current profile as modelled and reconstructed by IDE, with the non-inductive contributions colour-coded as in figure 2b) and the total reconstructed current density given by the solid black curve. Subtracting the former from the latter yields the dashed black line, i.e. the remaining ohmic current, which is of the same order as the uncertainties of the reconstructed current profile. As shown in figure 2c),  $q$  remains above 1.5 across the entire minor radius, which is supported by a lack of MHD activity of lower helicity. For higher  $\beta_N$ , ideal and resistive MHD instabilities with 2/1 helicity have been observed.

### Transport: Theory vs. Experiment

The understanding of plasma transport in non-inductive steady-state scenarios is an important requirement for realising advanced tokamaks. The plasma transport in the high- $\beta$  phase described above, which is several energy confinement times  $\tau_E$  long, was, therefore, modelled using ASTRA and TGLF [9, 10]. Electron temperature profiles can be reproduced well, whereas predicted ion temperature profiles deviate from the experiment in the high- $\beta$  phase. This is shown in figure 3: since the predicted  $\chi_i$  profile is significantly higher than the profile inferred from the experiment over a large part of the minor radius,  $R/L_{T_i}$  is likewise reduced, which results in a significantly lower core  $T_i$ . This is in contrast to previous results that found TGLF to accurately predict  $T_i$  in low- $\beta$  cases [11]. This shortcoming at high  $\beta$  cannot be resolved by

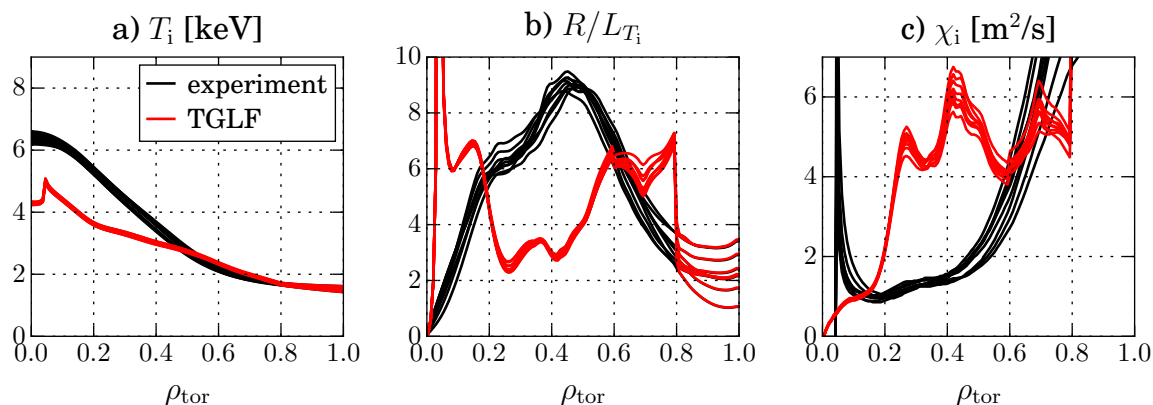


Figure 3: a) Ion temperature, b) normalised ion temperature gradient and c) ion heat diffusivity profiles as derived from a power balance analysis of the experiment (black) and as predicted by TGLF [10] (red) for 3.5 to 4.0 s in discharge 32303.

varying TGLF's input quantities within their uncertainties, e.g.  $q$ -profile, heating power or fast ion density. In particular the shape of the experimental  $T_i$  profile cannot be matched in this way. Since TGLF is based on quasi-linear calculations, this hints at a purely non-linear effect.

As a remark, a potential explanation is given by [12] where full gyrokinetic simulations of ion heat transport show that including electromagnetic effects from fast ions can improve ion heat confinement by up to  $\Delta(R/L_{T_i}) \approx 2$ . The discrepancy reported above (cf. figure 3b) is of the same order and the fast ion density is non-negligible at about 25% of the electron density ( $n_e \approx 5 \times 10^{19} \text{ m}^{-3}$ ), which is why similar gyrokinetic simulations are planned to investigate this explanation.

## References

- [1] J. Hobirk *et al.*, Plasma Physics and Controlled Fusion **54**, 095001 (2012)
- [2] Y. Sakamoto *et al.*, Nuclear Fusion **49**, 095017 (2009)
- [3] C. C. Petty *et al.*, Nuclear Fusion **56**, 016016 (2016)
- [4] A. Bock, PhD Thesis LMU München, IPP report 1/357 (2016)
- [5] R. Fischer *et al.*, this Conference, P1.016
- [6] R. Fischer *et al.*, Fusion Science and Technology **69**, 526–536 (2016)
- [7] R. T. Mumgaard and S. D. Scott, PSFC/JA-15-28 (2015)
- [8] D. Rittich *et al.*, this Conference, O4.134
- [9] G. Pereverzev and P. N. Yushmanov, IPP report 5/98 (2002)
- [10] G. M. Staebler *et al.*, Physics of Plasmas **14**, 055909 (2007)
- [11] F. Sommer *et al.*, Nuclear Fusion **55**, 033006 (2015)
- [12] J. Citrin *et al.*, Plasma Physics and Controlled Fusion **57**, 014032 (2015)

This work has been carried out within the framework of the EUROfusion Consortium and has received funding from the Euratom research and training programme 2014–2018 under grant agreement no. 633053. The views and opinions expressed herein do not necessarily reflect those of the European Commission.